Insulation Properties and Degradation Mechanism for XLPE Subjected to Different Aging Periods

Qian Wang, Rui Liu, *Student Member*, Sichen Qin, Xi Chen, Zicai Shen, Zhe Hou, and Zeli Ju

***Abstract*—Due to its excellent insulation and mechanical properties, cross-linked polyethylene (XLPE) is widely used as the insulation candidate of power cables in power transmission and distribution systems. However, its performance can be affected due to various stresses, which endangers safe operation of the power system in service. In this paper, dielectric and insulation properties of XLPE materials of 110 kV cables with the service lives of 0, 15, and 30 years were tested and evaluated. Results show that with increase of service life, dielectric loss caused by the polarization process increases significantly, and dielectric strength decreases as well. Power frequency breakdown field strength and crystallinity decrease significantly, and carbonyl index increases. The degradation process of XLPE can be divided into two stages: the structure of the crystalline region of the original sample is relatively complete, and loss can be almost ignored. After long-term service, the crystallization region is destroyed, and thermal oxygen reaction occurs. Intermolecular force is weakened, which makes breakdown easier to occur. However, there is no direct relation between the carbonyl index and macroscopic characteristics. This paper reveals the deterioration law of the XLPE cable insulation, which provides a theoretical basis for evaluating cable aging condition and is of great significance to improve cable operation safety and maintenance quality.**

***Index Terms*—Crosslinked polyethylene, dielectric properties, insulation performance, microstructure, power frequency breakdown.**

I. Introduction

THE cross-linked polyethylene (XLPE) has good insulation, heat resistance, and mechanical properties, and has become first choice of main insulation material of high voltage cable [1]. Under actual operation conditions, the cable may be damaged due to high temperature, high voltage, and high humidity, which probably leads to insulation failure. On September 29th, 2015, a cable in Dongguan failed due to insulation aging for 13 years after its first operation [2]. On February 15, 2021, the Texas power grid of the United States failed due to surge of power load, resulting in a large area power outage [3]. According to statistics, failure ratio caused by aging of insulation materials reaches 85.5% excepting external force failures [4].

During service of XLPE cable, due to influence of electric field, temperature field, and stress, aging of XLPE leads to an irreversible deterioration [5], [6]. Dielectric properties of XLPE have a specific relation with degradation degree [7]. C. Kim *et al*. tested dielectric properties of XLPE with different aging degrees under high-frequency electric fields. Results showed a loss peak in 4–8 MHz, which moves to a high-frequency direction with increase of aging time and its value was increased [8]. H. M. Wang *et al*. measured dielectric loss, oxidation induction time, and breakdown voltage of insulation samples in five kinds of 220 kV XLPE cables with different operating years. Results showed with increase of service life, dielectric loss gradually increases, and oxidation induction period of insulation is shortened. When the cable runs for 5–12 years, barrier voltage is significantly reduced [9]. L. A. Dissado *et al*. found that crystallinity, content of crosslinking by-products, and internal mechanical stresses of the XLPE in cables are different at different radial positions, and physical and chemical properties of XLPE in different radial positions may cause difference in their breakdown performances [10]. G. C. Montanari used differential scanning calorimetry (DSC) to test oxygen stability of aged XLPE, PP, and other insulation materials. Results showed the activation entropy of each sample during oxidation showed a linear relation with enthalpy [11]. J. L. He *et al*. showed chemical degradation of XLPE during electrical aging might destroy the intrinsic healing function of the insulation [12]. H. Li and J. Y. Li conducted an accelerated thermal aging test on a commercial 110 kV XLPE cable insulation. They found the thermal aging process was divided into physical and chemical aging stages according to whether the antioxidant was consumed. In the physical aging stage, recrystallization process makes the imperfect crystals perfect, and crystallinity increases. In the chemical aging stage, the molecular chain of XLPE was broken, and crystallinity decreased due to oxidation reaction [13]. B. X. Du *et al*. studied insulation characteristics of 14 110 kV and 220 kV XLPE cables by thermogravimetry, infrared spectroscopy, and other methods. It was found that four deteriorated, such as lower initial decomposition temperature, higher carbonyl index, etc. Insulation degradation would be accelerated if they were subjected to excessive fault current impact or external high

Manuscript received August 19, 2021; revised September 26, 2021; accepted October 23, 2021. Date of online publication December 9, 2022; date of current version July 19, 2023. This work was supported by the National Natural Science Foundation of China under Grant No. 11975052, 51507135, 52107029. This work was also supported by China Postdoctoral Science Foundation (No. 2021M692599).

Q. Wang, R. Liu, S. C. Qin (corresponding author, email: qinsc31@163.com; ORCID: https://orcid.org/0000-0002-4630-534X), and X. Chen are with the Department of Electrical Engineering, Xi'an University of Technology, Xi'an 710048, China.

Z. C. Shen is with the Beijing Institute of Spacecraft Environment Engineering, Beijing 100094, China.

Z. Hou and Z. L. Ju are with the State Grid Shaanxi Electric Power Research Institute, Xi'an 710100, China.

DOI: 10.17775/CSEEJPES.2021.06140

2096-0042 © 2021 CSEE. This is an open access article under the CC BY-NC-ND license (http://creativecommons.org/licenses/by-nc-nd/4.0/).

temperature [14]. Y. Yin *et al*. conducted DC breakdown and space charge tests on XLPE samples with different thicknesses at 30, 50, and 70°C. Results showed the breakdown field strength of XLPE decreases with increase of temperature, and the relation between breakdown field strength and thickness of XLPE at different temperatures conforms to the inverse power law [15]. M Tefferi, *et al*. showed that crosslinking process can significantly improve thermal and mechanical properties of polyethylene, but residual crosslinking by-products may act as impurities and seriously affect performance of crosslinked polyethylene cables. It is also found a large amount of space charge accumulation in XLPE will lead to field enhancement in the process of polarity reversal [16].

At present, a large number of scholars have done a lot of research on cable degradation from different aspects. However, the essential cause of aging needs to be further explored. It can be seen that aging of cable insulation is reflected in short-range structure such as chemical groups, and affects long-range structure such as crystallization and cross-linking. Therefore, this paper studies the dielectric properties, macro insulation properties, and microstructure of the XLPE used in power electric cables, and reveals the deterioration mechanism of XLPE insulation which serves as a basis for evaluation of material deterioration.

II. Sample Preparation and Test Methods

A. Sample Preparation

Samples are from XLPE cables retired from a 110 kV power transmission line of China Southern Power Grid Corporation, these cables have been running for 0, 15, and 30 years, and these samples were labeled as S_0, S_15, and S_30, respectively. Production time and specifications of the three cables are the same. All samples are picked from insulation that is close to the inner shielding layer and the corresponding schematic diagram is shown in Fig. 1.

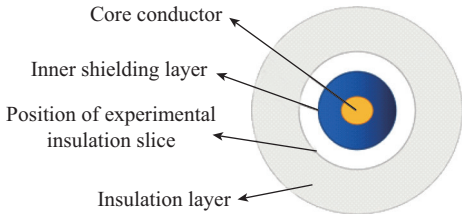


Fig. 1. The schematic diagram of XLPE cable insulation cutting.

Thickness of the three groups of slice samples is about 0.3 mm; the sliced sample is shown in Fig. 2. They are cut into the shape of the applicable test system. Wipe the sample with alcohol, remove surface impurities, and conduct test after drying.

B. Broadband Dielectric Spectrum (BDS) Test

A German Novocontrol concept 40 broadband dielectric spectrometer was used for the dielectric spectrum test. Test was carried out in N_2 atmosphere, with a frequency range of 0.1–10^6 Hz and a temperature range of $-100\sim100$°C with a step size of 20°C. Test of each sample was performed twice to ensure accuracy of the data.

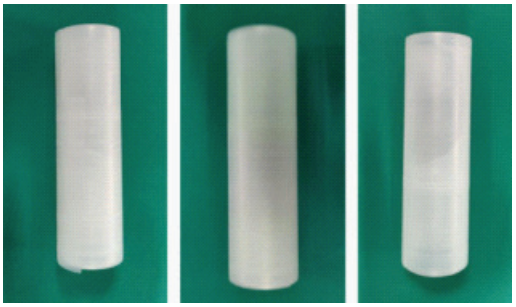


Fig. 2. Sliced samples of XLPE.

C. Power Frequency Breakdown Test

A HCDJC-50 kV breakdown testbed was used for the power frequency breakdown test of 10 × 10 cm sliced sample. Test procedure was based on the GB 1408-2006. Input voltage is AC, and boost rate was 1 kV/s. Two samples were used from each test group, and five test points were selected from each group, and 10 effective values were recorded.

D. Fourier Transform Infrared Spectroscopy (FTIR) Test

The infrared spectrum tester adopted the American thermophilic Nicolet Is50 infrared spectrometer, with resolution of 0.09 cm^{-1}, spectral range of 27000∼15 cm^{-1}, signal-to-noise ratio 55000:1, and wavenumber accuracy of better than 0.005 cm^{-1}.

E. Differential Scanning Calorimetry (DSC) Test

Differential scanning calorimeter was performed by using a 200 F3 type differential scanning calorimeter made by Netzsch. The experiment was carried out in N_2 atmosphere, the temperature range was 30–200°C, and the heating and cooling rates were 10°C/min.

III. Test Result

A. Results of Broadband Dielectric Spectrum

1) The Real Part of the Dielectric Constant

Variation of the real part of the dielectric constant of XLPE samples as a function of temperatures and frequencies is shown in Fig. 3.

It can be seen from Fig. 3 that at fixed temperatures, the dielectric constant of the three samples shows a decreasing trend with increase of frequency. At power frequency, when temperature is lower than room temperature, dielectric constant of S_0 increases with increase of temperature. However, this value decreases with increase of temperature above room temperature. For S_15, the growth rate of dielectric constant below −70°C is higher than at $-70\sim100$°C, where this value remains at merely 8% at 50 Hz. There is a significant inflection point at 10^5 Hz. In the high-frequency region, with increase of temperature, dielectric constant first increases and then slightly decreases.

2) The Tangent Value of the Dielectric Loss Angle

Tangent values of XLPE samples at different temperatures and frequencies can be found in Fig. 4. There are one loss peak and one relaxation peak around 1 Hz and $10\sim10^3$ Hz for S_0,

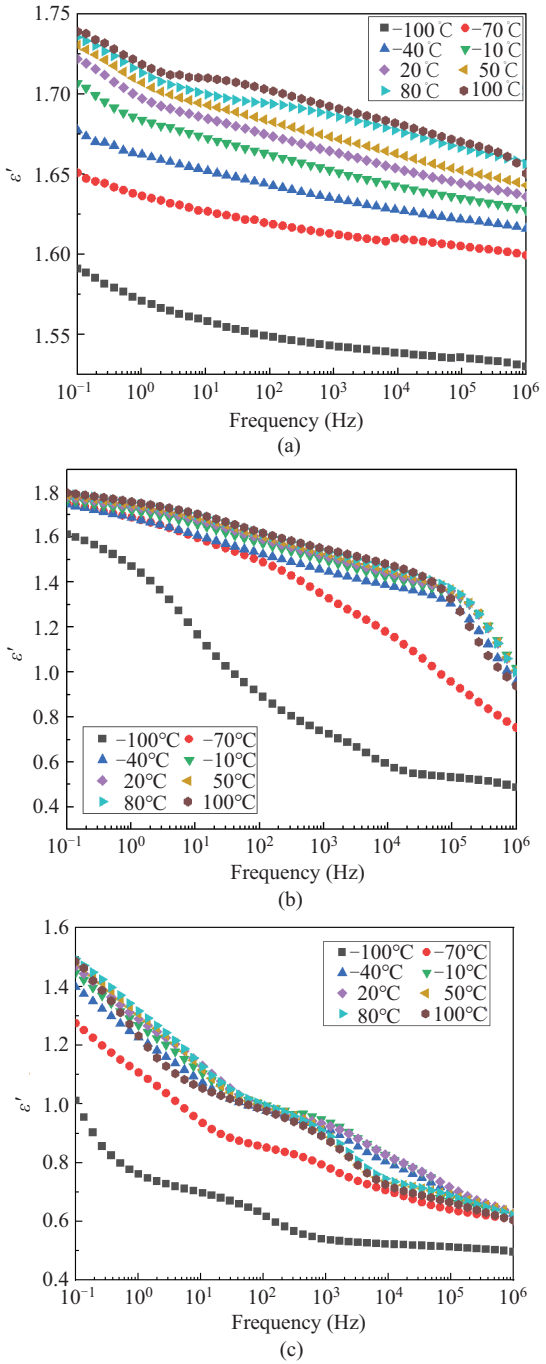


Fig. 3. Real part of dielectric constant of samples. (a) Real part of dielectric constant of S_0. (b) Real part of dielectric constant of S_15. (c) Real part of dielectric constant of S_30.

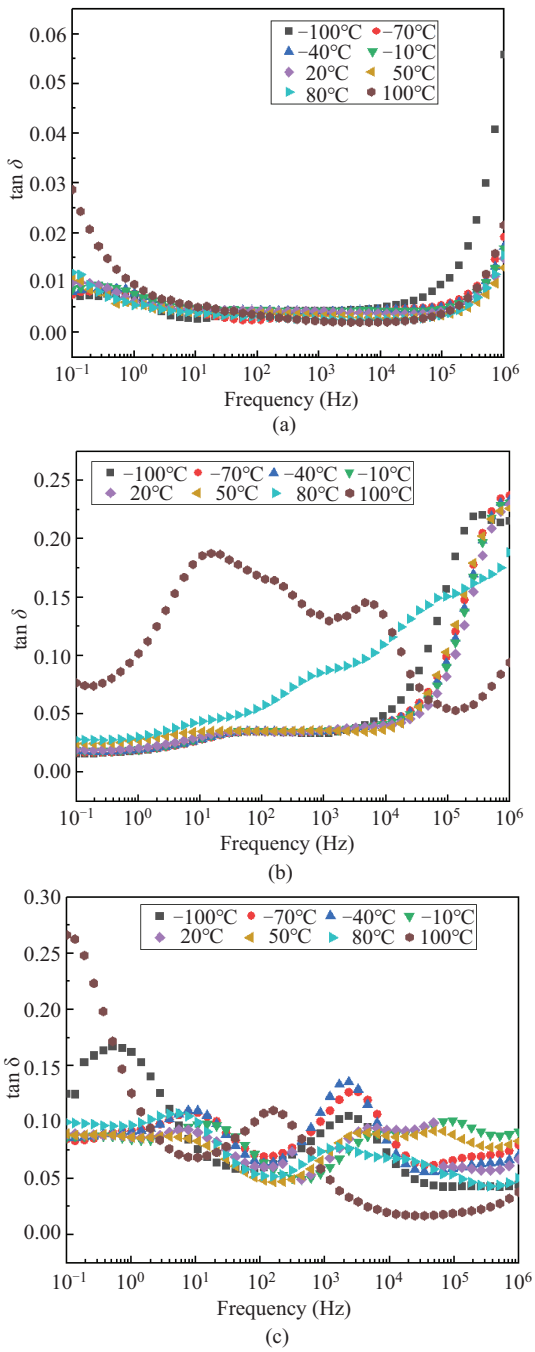


Fig. 4. Dielectric loss of samples. (a) Dielectric loss of S_0. (b) Dielectric loss of S_15. (c) Dielectric loss of S_30.

and they gradually move to the direction of high temperature and high-frequency with increase of temperature. Moreover, maximum dielectric loss of S_0 appears at low temperature and high-frequency region, which is nearly 0.056. A loss peak with a low amplitude can be observed in the frequency band of 10∼10^3 Hz for S_0, which moves slightly to the low frequency direction with increase of temperature. Loss peak near 10^5 Hz gradually moves to high temperature and high-frequency direction with increase of temperature (which is beyond test range), as well. On the whole, dielectric loss of the S_15 increases significantly both at high temperatures and at high-frequency regions. For S_30, maximum dielectric loss of the sample reaches 0.27, and the number of the loss peaks increases, as well. There are two loss peaks with high amplitude at 1 Hz and 10^3–10^4 Hz, and three loss peaks with low amplitude can be observed at 10^5–10^6 Hz, which occur at −70°C, −10°C, and 50°C, respectively. Loss peak amplitude increases with increase of frequency.

3) The Conductivity of Samples

The dielectric loss tangent can be expressed as the ratio of leakage current to charging current, as shown in (1):

$$\tan\delta = \frac{I_{\rm l}}{I_c} = \frac{G(\omega)U}{\omega C(\omega)U} = \frac{G(\omega)}{\omega C(\omega)} \tag{1}$$

where $C(\omega) = \varepsilon'_{\rm r}C_0$, C_0 is defined as vacuum capacitance, $\varepsilon'_{\rm r}$ is the real part of the relative dielectric constant, $G(\omega)$ is conductance.

Conductivity of sample calculated by the above formula is shown in Fig. 5. It can be seen after frequency reaches 10^5 Hz, conductivity of S_0 shows an upward trend with increase of frequency, and is basically not affected by temperature. Conductivity of S_15 begins to rise when frequency exceeds 10^4 Hz but does not reach 10^5Hz, and rising range increases. It is more affected by temperature under high temperature. For S_30, the above phenomenon appeared when frequency is 10^4 Hz. Generally speaking, conductivity is related to carrier concentration, carrier mobility and amount of charge carried by carriers. With increase of frequency and temperature, combined action of electric field and heat leads to chain breaking of molecular chain, side chain and short chain, resulting in some non-polar small molecular groups, and the number of shallow traps in the sample increases. Carriers jump between these shallow traps to form jump conductance, so conductivity increases.

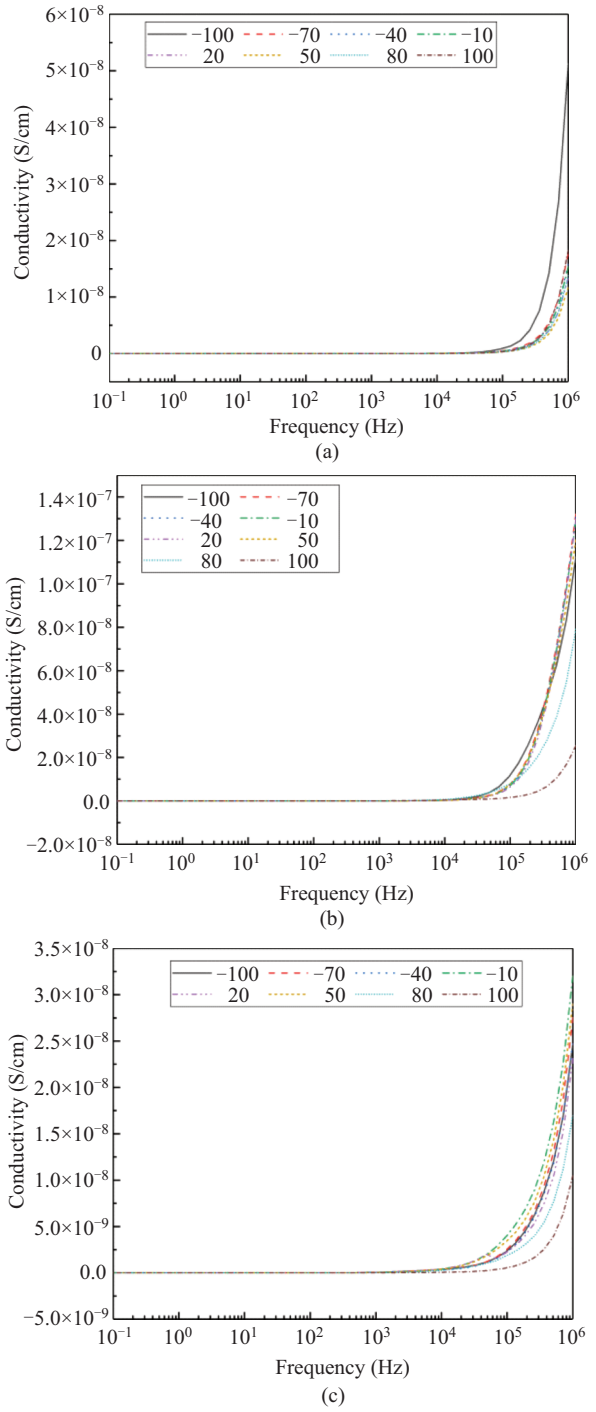


Fig. 5. Conductivity of samples. (a) Conductivity of S_0. (b) Conductivity of S_15. (c) Conductivity of S_30.

4) The Relaxation Activation Energy

Relaxation activation energy can characterize the difficulty of relaxation polarization [17]. In this paper, relaxation activation energy of XLPE cable samples with different service lives is calculated by the Arrhenius equation [18]. The generalized expression is as follows:

$$f_{\max} = \varphi_0 \exp\left(\frac{E_{\rm a}}{{\rm R}T}\right) \tag{2}$$

where $f_{\max}$ is frequency factor, ϕ_0 is frequency factor, R is gas constant with a value of 8.314 J/(mol·K), $E_{\rm a}$ is relaxation activation energy.

Frequency $f_{\max}$ corresponding to peak value of the dielectric loss at different temperatures is extracted from dielectric spectrum test data, and obtained results are fitted linearly, as shown in Fig. 6.

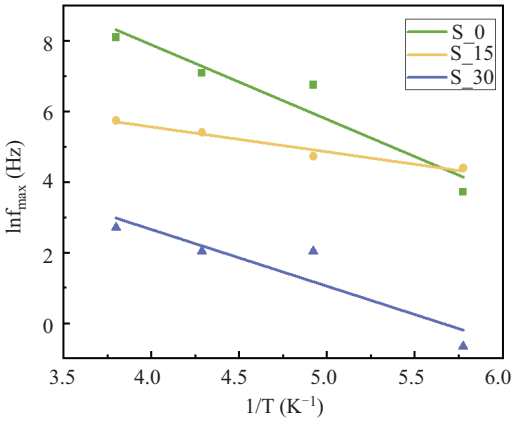


Fig. 6. Linear fitting of activation energy of samples.

Relaxation activation energy can be obtained by multiplying the slope of the fitting line by R. Specific calculation results are shown in Fig. 7. With increase of service life, relaxation activation energy of samples shows a trend of first decreasing then increasing.

B. Results of the Power Frequency Breakdown

The Weibull distribution mathematical statistics method is used to process data [19]. The expression of two-parameter Weibull distribution function is as follows:

$$F(x) = 1 - \exp\left[-\left(\frac{x}{\alpha}\right)^{\beta}\right] \tag{3}$$

where x is breakdown field strength obtained from the test, kV/mm, α is characteristic breakdown field strength (scale parameter), β is shape parameter. Take logarithms on both sides of the equal sign of equation 3. Draw after processing power frequency breakdown experimental data. That is, the abscissa is the logarithm of breakdown field strength.

The Weibull distribution of breakdown field strength of the XLPE samples is shown in Fig. 8. Distribution of the three samples is approximately a straight line. Power frequency breakdown parameters of the three samples are shown in Table I. When failure probability is 63.2%, breakdown field strength of S_0 shows the highest value, which is 25.58 kV/mm. The breakdown field strength of the S_15 and S_30 decreased by 16.0% and 16.4% compared with S_0.

C. Results of the Fourier Transform Infrared Spectroscopy

Infrared spectrum of samples is shown in Fig. 9. There are four characteristic absorption peaks in the figure, which are 718 cm^{-1}, 1470 cm^{-1}, 2848 cm^{-1}, and 2951 cm^{-1}, respectively. Compared with the infrared spectrum characteristic library, they are all methylene (–CH_2–) vibration absorption peaks under different vibration modes. They are –CH_2– plane rocking vibration, –CH_2– variable angle vibration peak, –CH_2– symmetric stretching vibration peak and –CH_2– antisymmetric stretching vibration peak, respectively.

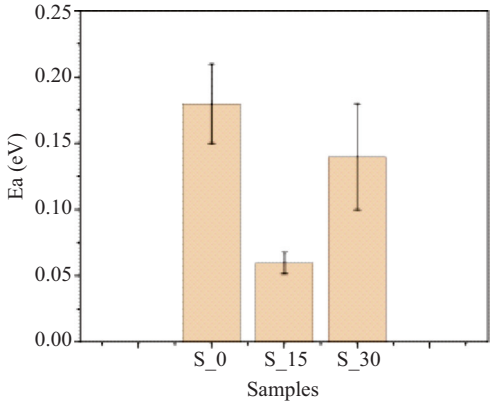


Fig. 7. Activation energy diagram of samples.

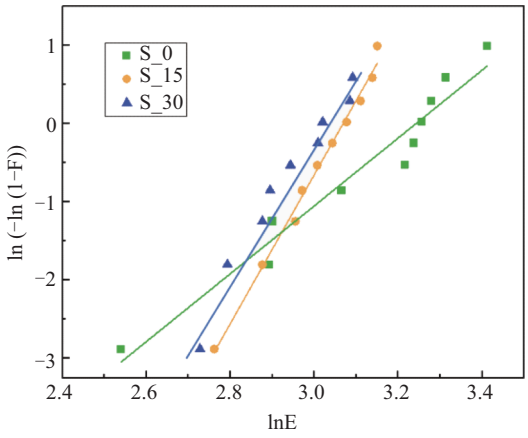


Fig. 8. Weibull distribution of breakdown strength of samples.

TABLE I
THE POWER FREQUENCY BREAKDOWN PARAMETERS OF XLPE SAMPLES

Sample	Scale parameter (α)	Shape parameter (β)
S_0	25.58	4.34
S_15	21.51	9.51
S_30	21.39	6.52

During long-term service of the cable, the residual crosslinking agent in the cable will be decomposed into acetophenone, cumyl alcohol, and sodium hydroxide α-Methyl styrene and other products [20]. When phenolic and sulfur antioxidants are added to XLPE, aging of the polymer will be significantly inhibited [21], [22]. In order to further judge thermal oxygen degradation degree of the three samples, the peak area of 1600–1800 cm^{-1} is used to characterize the carbonyl index of the three samples [23]. Local spectrum is shown in Fig. 10.

It can be seen from Fig. 10 the carbonyl index of S_0 has a higher value, which is due to S_0 is in nonoperating state, without the effect of high temperature and electric field, the additives decomposed in the sample cannot be volatilized. The carbonyl index of S_15 is the highest. This is due to the thermo oxygenation reaction under the electrothermal stresses. At such conditions related thermos-oxygenation by-products are produced, and the molecular chain is broken, resulting in oxidized side chains. It also shows that antioxidants have been consumed and have no good inhibition on oxidation

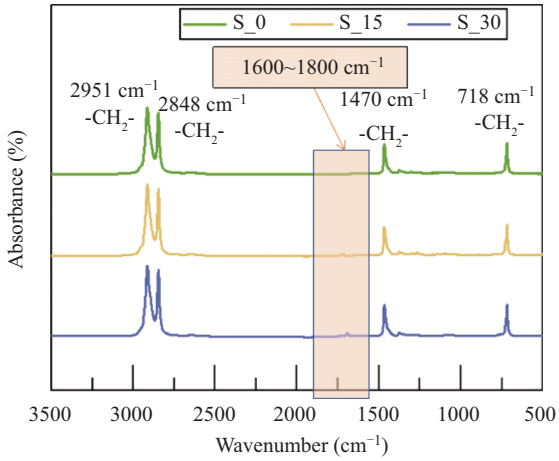


Fig. 9. The infrared spectrum of samples.

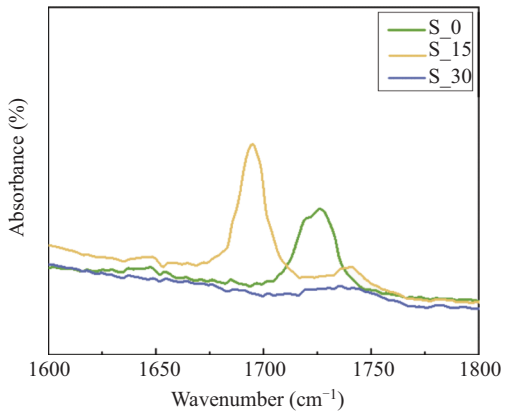


Fig. 10. Partial infrared spectra of samples.

and carbonyl formation in the aging process [24]. After long-term service, internal impurities have been consumed, which is mainly due to destruction of macromolecular chains, resulting in increase of small molecular chains and oxygen intrusion.

D. Results of the Differential Scanning Calorimetry

DSC melting curves of samples is shown in Fig. 11. Melting enthalpy is calculated from the DSC peak area measured in Fig. 11, crystallinity of the three samples is calculated according to formula (4), as shown in Table II.

$$\chi = \frac{\Delta H_{\mathrm{m}}}{\Delta H_{100}} \times 100\% \tag{4}$$

where χ is crystallinity (%), $\Delta \mathrm{H_m}$ is melting enthalpy (J/g), $\Delta \mathrm{H_{100}}$ is crystallization enthalpy with 100% crystallinity, usually taken as $\Delta \mathrm{H_{100}} = 291$ J/g.

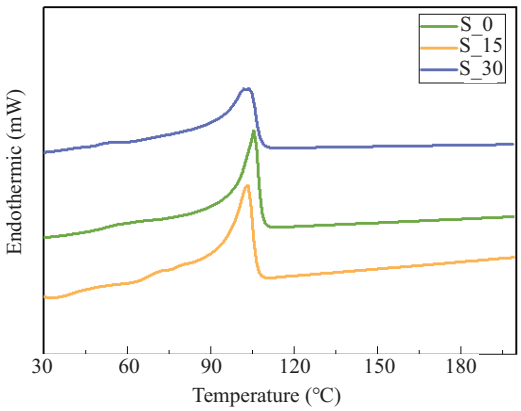


Fig. 11. The DSC melting curve of samples.

TABLE II
CRYSTALLINITY OF XLPE SAMPLES

Sample	S_0	S_15	S_30
Crystallinity χ (%)	23.7	19.6	18.8

Due to insulation deterioration, the XLPE macromolecular chain in the crystallization zone is seriously damaged, resulting in decrease of crystallinity.

IV. DISCUSSION

A. The Relation Between the Molecular Structure and the Dielectric Properties

Impurities in cable insulation gradually volatilize due to the long-term effect of operating temperature [25], and some polar impurities would adhere to the XLPE macromolecular chain. In the low-frequency band, the polar group or molecular chain relaxes and polarized under the electric field, and the polar molecular chain can keep up with change of the electric field frequency. With increase of the electric field frequency, the polar groups attached to the macromolecular chain cannot keep up with electric field variation at high frequencies, and dielectric relaxation phenomenon occurs [26], which reduces relative dielectric constant. In addition, thermal movement of the polar groups occurs with increase of temperature, which further prevents polar molecules from being bounded by the electric field [27]. Therefore, in high-frequency region, relative permittivity first increases and then slightly decreases with increase of the temperature.

According to the temperature dependence theory of dielectric loss, relaxation polarization can be divided into three relaxation processes according to temperature [28], which include α, β and γ. γ relaxation mainly occurs at low or high temperature, and corresponding vibration frequency is above 10^{12} Hz. β relaxation occurs in a broad temperature frequency domain between α and γ relaxation, while α relaxation generally occurs in high temperature and low-frequency regions [29]. The three samples have different degrees of relaxation polarization. Peak loss of S_0 caused by γ relaxation is 0.056. For S_15, γ relaxation increases significantly, up to 0.237. However, peak value of S_30 decreases only by 0.08. The main reason for increase of γ relaxation peak value of S_15 is crosslinking by-products increased, and most of them existed in the amorphous region, which was reflected in the relaxation process. γ relaxation peak value of S_30 decreases because the network structure composed of short-chain cross-linking restricts movement of small molecular chains, which leads to formation of small molecular chains.

β relaxation exists in S_0 at $-20\sim$-100°C and 1 Hz, with a peak of 0.008. With increase of temperature, β relaxation can well exist at 10^6 Hz, and corresponding peak value increases to 0.021. β relaxation occurs in S_15 at the low-temperature region of medium frequency and medium-temperature region of high-frequency. β relaxation at high-frequency is no longer a single relaxation process, and its peak loss is about 0.23. For S_30, β relaxation is weakened. At low-temperature, low-frequency, and medium-frequency β relaxation represents movement of different polar groups or local segments, and peak losses are 0.167 and 0.136, respectively. It can be found β relaxation loss first increases and then decreases with long-term service.

At 100°C and 0.1 Hz, α relaxation exists in all samples, with peak values being 0.029, 0.076, and 0.266, respectively. Slow secondary cross-linking reaction takes place in XLPE-insulated cables at service, which makes α relaxation loss increase gradually with time [30]. Degradation of XLPE insulation results in an increase of amorphous area in the lamellae, which provides more free space for movement of the main chain and makes stable α relaxation more likely to occur.

According to the previous analysis, samples have deteriorated to a certain extent during the past 15 years. Short-chain cross-linking in the amorphous region and increase of impurities such as cross-linking by-products have led to introduction of more polar groups. That makes β relaxation polarization occurrence more likely [31]. Due to volatilization of impurities and secondary crosslinking, relaxation activation energy of S_30 is increased. Because the main chain of the insulation in the long-term service cable has been seriously damaged, secondary crosslinking is not enough to make up for dielectric properties contributed by the complete structure of the macromolecular chain. As a result, relaxation activation

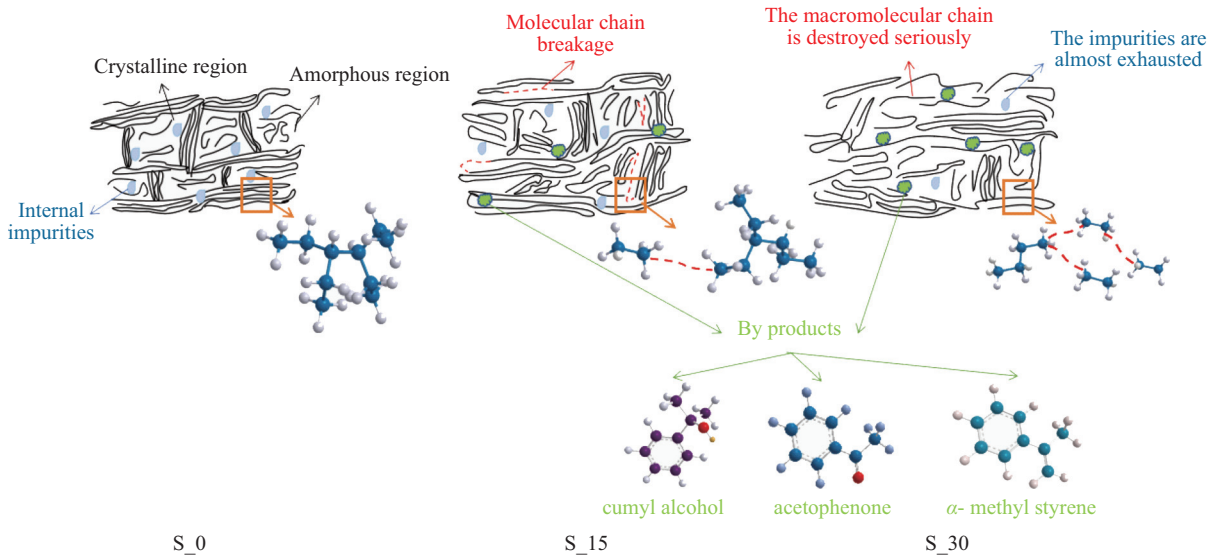


Fig. 12. Schematic diagram of microstructure deterioration of XLPE.

energy of S_30 is still lower than S_0's. The schematic diagram of structural deterioration is shown in Fig. 12.

B. The Relation Between the Molecular Structure and the Insulation Performance

The carbonyl index of the samples obtained from the FTIR shows the carbonyl index of S_15 is highest, which means thermal oxygen aging of the insulation is the most serious. However, from the power frequency breakdown test, it is found that breakdown field strength of S_15 is not lowest, which indicates the carbonyl index cannot directly explain change of breakdown characteristics. According to DSC test, crystallinity of S_0 is highest, and crystal structure of S_0 is relatively complete and orderly compared with the other two samples. Therefore, it can be confirmed the carbonyl group in S_0 mainly exists in the amorphous region. XLPE is a polymer material with both amorphous and crystalline regions [32], and deterioration of crystalline region is the direct manifestation of insulation deterioration.

Holes injected by the electrode mainly migrate and transport on macromolecular chains of XLPE, while electrons tend to migrate between macromolecular chains. Because of the van der Waals force between XLPE molecular chains [33], migration of electrons are not continuous, and the charge transport can be completed only by crossing different barriers. From power frequency breakdown test results, it is found that with increase of service time, breakdown field strength gradually decreases. This is because cracking of the XLPE macromolecular chain weakens the force among molecular chains. Recrystallization produces more interfaces for migration of electrons in the sample, which reduces obstacles and makes breakdown occur easier.

V. Conclusion

In this paper, XLPE samples from cables that have been operated for 0, 15, and 30 years at site were used for experimental research. Dielectric and insulation properties of the samples were tested, and molecular structure characteristics were studied based on FTIR and DSC tests. The degradation mechanism of dielectric and insulation properties was analyzed. Conclusions are as follows:

1) dielectric constant of S_0 shows the largest value. Maximum dielectric loss and the breakdown field strength of the S_0 are 0.056 and 25.58 kV/mm, respectively. After long-term operation, the dielectric constant of the cable increased first and then decreased slightly. The number of loss peaks increased and peak value increased, with its maximum value reaching 0.27. Breakdown field strength of S_15 and S_30 decreased by 16.0% and 16.4%, respectively, but the carbonyl index of the sample after 15 years of operation was highest. Evolution of molecular structure was analyzed by FTIR and DSC from short-range structure and long-range structure, respectively. Results show crystallinity of S_0 was 23.7%, and a large number of carbonyl products were produced in long-term operation cables. Crystallinity of S_15 and S_30 decreased to 19.6% and 18.8%, respectively.

2) With increase of service life, the XLPE main chain was broken, resulting in increase of amorphous region. The structure of the crystalline region becomes loose, and local and whole molecular segments of the macromolecular chain are easier to move. The whole molecular chain segment, increase of polar small molecular substances in the sample, and significant increase of dielectric loss are caused by polarization process. In addition, recrystallization increased the interface, which reduced the obstacle of the electron migration in the sample, resulting in decrease of dielectric strength. Decrease of the crystallinity of the sample and the increase of carbonyl content in the crystallization area were the direct manifestation of cable deterioration at the micro level. Carbonyl index of S_15 was highest, but breakdown field strength was not lowest, indicating the carbonyl index can characterize the degree of thermal oxygen aging, but it was not directly related to macro performance.

REFERENCES

[1] B. X. Du, C. L. Han, J. Li, and Z. L. Li, "Research status of polyethylene insulation for high voltage direct current cables," *Transactions of China Electrotechnical Society*, vol. 34, no. 1, pp. 179–191, Jan. 2019.

[2] S. C. Huang, "Dongguan city Guancheng district of 10kV distribution system reliability research," M.S. thesis, Department, South China University of Technology, Guangzhou, 2017.

[3] X. M. An, H. D. Sun, X. H. Zhang, L. Y. Ji, W. M. Sun, J. Z. Tu, J. He, and Q. Y. Zhou, "Analysis and lessons of texas power outage event on February 15, 2021," *Proceedings of the CSEE*, vol. 41, no. 10, pp. 3407–3415, May 2021.

[4] B. J. Hui, M. L. Fu, T. Liu, S. Hou, C. Liu, and J. M. Guo, "Statistical analysis on failures of 110 kV and above power cable system," *Southern Power System Technology*, vol. 11, no. 12, pp. 44–50, 67, Dec. 2017.

[5] M. G. Andersson, M. Jarvid, A. Johansson, S. Gubanski, M. R. S. Foreman, C. Müller, and M. R. Andersson, "Dielectric strength of γ-radiation cross-linked, high vinyl-content polyethylene," *European Polymer Journal*, vol. 64, pp. 101–107, Mar. 2015.

[6] R. Ullah and M. Akbar, "Lifetime Estimation Based on Surface Degradation and Characterization of HTV Silicone-rubber Based Composites for HVAC and HVDC Transmission," *CSEE Journal of Power and Energy Systems*, vol. 9, no. 2, pp. 751–758, Mar. 2023.

[7] Y. Liu, L. J. Wang, Y. Su, Y. Xiao, and X. L. Cao, "Ageing condition assessment of XLPE cable insulation based on $\tan\delta$ at 0.1 Hz," *Insulating Materials*, vol. 49, no. 5, pp. 41–45, May 2016.

[8] C. Kim, Z. J. Jin, P. K. Jiang, Z. S. Zhu, and G. L. Wang, "Investigation of dielectric behavior of thermally aged XLPE cable in the high-frequency range," *Polymer Testing*, vol. 25, no. 4, pp. 553–561, Jun. 2006.

[9] H. M. Wang, S. C. Fang, Z. Z. Meng, P. X. Song, X. Li, M. Z. Zhu, X. H. Zhu, Y. Yu, and B. X. Du, "Dielectric properties of high voltage XLPE power cables taken from service," in *Proceedings of 2019 IEEE Conference on Electrical Insulation and Dielectric Phenomena (CEIDP)*, Richland, WA, USA, 2019, pp. 186–189.

[10] L. A. Dissado, J. C. Fothergill, A. See, G. C. Stevens, L. Markey, C. Laurent, G. Teyssedre, U. H. Nilsson, G. Platbrood, and G. C. Montanari, "Characterizing HV XLPE cables by electrical, chemical and microstructural measurements on cable peeling: Effects of surface roughness, thermal treatment and peeling location," in *Proceedings of 2000 Annual Report Conference on Electrical Insulation and Dielectric Phenomena (Cat. No. 00CH37132)*, Victoria, BC, Canada, 2000, pp. 136–140.

[11] G. C. Montanari, A. Motori, A. T. Bulinski, S. S. Bamji, and J. Densley, "Application of oxidation induction time and compensation effect to the diagnosis of HV polymeric cable insulation," *IEEE Transactions on Dielectrics and Electrical Insulation*, vol. 3, no. 3, pp. 351–360, Jun. 1996.

[12] Y. Yang, Z. M. Dang, Q. Li, and J. L. He, "Self-healing of electrical damage in polymers," *Advanced Science*, vol. 7, no. 21, pp. 2002131, Nov. 2020.

[13] H. Li, J. Y. Li, Y. X. Ma, and Q. M. Yan, "Effects of thermal aging on the crystal structures of the XLPE cable insulating material at different temperatures," *Proceedings of the CSEE*, vol. 37, no. 22, pp. 6740–6748, Nov. 2017.

[14] L. Wang, B. X. Du, and Z. G. Ren, "Test and analysis of insulation deterioration of XLPE power cable," *High Voltage Engineering*, vol. 40, no. 1, pp. 111–116, Jan. 2014.

[15] K. Y. Qian, P. F. Su, J. D. Wu, and Y. Yin, "The effect of thickness on breakdown strength in high voltage direct current cable insulation at different temperatures," *Proceedings of the CSEE*, vol. 38, no. 24, pp. 7121–7130, Dec. 2018.

[16] M. Tefferi, Z. Z. Li, H. Uehara, Q. Chen, and Y. Cao, "Characterization of space charge and DC field distribution in XLPE and EPR during voltage polarity reversal with thermal gradient," in *Proceedings of 2017 IEEE Conference on Electrical Insulation and Dielectric Phenomenon (CEIDP)*, 2017, pp. 617–620.

[17] Z. J. Shen, Z. Y. Luo, W. P. Zhan, T. B. Chen, X. L. Chu, Y. Y. Yu, B. H. Ouyang, and J. Y. Li, "Analysis on thermal aging behaviors of XLPE cable insulation based on trap parameters and relaxation process," *Proceedings of the CSEE*, vol. 36, no. 19, pp. 5382–5388, Oct. 2016.

[18] S. Morsalin and B. T. Phung, "Dielectric response measurement on service-aged XLPE cables: From very low frequency to power frequency," *IEEE Electrical Insulation Magazine*, vol. 36, no. 5, pp. 19–31, Sep./Oct. 2020.

[19] Z. Q. Liu, Z. Gao, J. Hao, H. P. Li, and Z. P. Ma, "Step breakdown characteristics and life model of AC 500 kV crosslinked polyethylene submarine cable insulating material," *Insulating Materials*, vol. 53, no. 2, pp. 29–35, Feb. 2020.

[20] Y. F. Zhao, Z. Z. Han, Y. Xie, X. H. Fan, Y. Y. Nie, P. Y. Wang, G. Liu, Y. P. Hao, J. S. Huang, and W. W. Zhu, "Correlation between thermal parameters and morphology of cross-linked polyethylene," *IEEE Access*, vol. 8, pp. 19726–19736, Jan. 2020.

[21] K. Hirota, Y. Kanemitu, N. Kamada, and Y. Sekii, "The influence of antioxidants on electrical tree generation in XLPE," *Electrical Engineering in Japan*, vol. 135, no. 3, pp. 1–7, May 2001.

[22] J. Zhai, W. Li, J. Zha, Q. Cheng, X. Bian and Z. Dang, "Space charge suppression of polyethylene induced by blending with ethylene-butyl acrylate copolymer," *CSEE Journal of Power and Energy Systems*, vol. 6, no. 1, pp. 152–159, Mar. 2020.

[23] Y. Y. Zhang, Z. K. Hou, K. N. Wu, S. H. Wang, J. Y. Li, and S. T. Li, "Influence of oxygen diffusion on thermal ageing of cross-linked polyethylene cable insulation," *Materials*, vol. 13, no. 9, pp. 2056, Apr. 2020.

[24] H. K. Lv, T. H. Lu, L. Q. Xiong, X. G. Zheng, Y. Y. Huang, M. L. Ying, J. C. Cai, and Z. Li, "Assessment of thermally aged XLPE insulation material under extreme operating temperatures," *Polymer Testing*, vol. 88, pp. 106569, Aug. 2020.

[25] A. X. Zhao, X. Chen, L. Xu, J. M. Li, J. B. Deng, and G. J. Zhang, "Application of dielectric response in diagnoses of time and frequency domain on XLPE cable insulation," *High Voltage Engineering*, vol. 46, no. 1, pp. 292–302, Jan. 2020.

[26] W. W. Li, W. Y. Zheng, L. L. Ren, H. Li, X. T. Zhao, C. Wang, and J. Y. Li, "A comparative study on the insulation ageing of 10 kV XLPE cable via accelerated electrical test and accelerated water tree test," *Journal of Electrical Engineering & Technology*, vol. 17, no. 1, pp. 475–484, Jun. 2022.

[27] T. L. Qiao, "Performance test and analysis of high voltage AC crosslinked polyethylene cable insulation," M.S. thesis, Department, Harbin University of Science and Technology, Harbin, 2019.

[28] K. C. Kao, *Dielectric Phenomena in Solids*. San Diego: Academic Press, 2004, pp. 573–581.

[29] S. C. Qin, Y. P. Tu, T. Tan, S. H. Wang, Z. K. Yuan, C. Wang, L. F. Li, and Z. X. Wu, "The effects of γ-ray on charging behaviour using polyimide," *Journal of Physics D: Applied Physics*, vol. 51, no. 24, pp. 245302, May 2018.

[30] L. Cao, L. S. Zhong, Y. E. Li, J. H. Gao, and G. O. R. G. Chen, "Crosslinking dependence of direct current breakdown performance for XLPE-PS composites at different temperatures," *Polymers*, vol. 13, no. 2, pp. 219, Jan. 2021.

[31] Z. M. Yan, K. Yang, Y. Y. Zhang, S. H. Wang, and J. Y. Li, "Crosslinking dependence of trap distribution and breakdown performance of crosslinked polyethylene," *Journal of Materials Science: Materials in Electronics*, vol. 30, no. 23, pp. 20605–20613, Nov. 2019.

[32] O. A. Lambri, F. G. Bonifacich, J. Á. García, E. D. V. Giordano, G. I. Zelada, F. A. Sánchez, R. R. Mocellini, and F. Plazaola, "Mechanical energy losses in commercial crosslinked low-density polyethylene in the temperature range between 200 and 400 K," *Journal of Applied Polymer Science*, vol. 136, no. 23, pp. 47605, Jun. 2019.

[33] L. Yang, L. Sun, and W. Q. Deng, "Van Der Waals function for molecular mechanics," *The Journal of Physical Chemistry A*, vol. 124, no. 10, pp. 2102–2107, Jan. 2020.



Qian Wang received her B.S. degree from Northeast Electric Power University in 2004, and her M.S. and Ph.D. degrees from North China Electric Power University in 2007 and 2012, respectively. Currently, she is an Associate Professor of the School of Electrical Engineering of Xi'an University of Technology, and also the deputy director of the Institute of High Voltage and Insulation Technology. Her current research interests include the insulation characteristics of dielectric materials in power systems and the insulation status detection of power grid equipment.



Rui Liu received her B.S. degree from Xi'an University of Technology in 2021. Currently, she is working toward her M.S. degree in Xi'an University of Technology. Her research interests include the insulation characteristics of dielectric materials in power systems and the insulation status detection of power grid equipment.



Zicai Shen received a Ph.D. degree from the Shanghai Institute of Optics and Precision Mechanics, Chinese Academy of Sciences. Currently, he is a researcher in Beijing Institute of Spacecraft Environment engineering, and is engaged in spacecraft space environment engineering and aerospace material engineering.



Sichen Qin received his B.S. and Ph.D. degrees from North China Electric Power University in 2015 and 2020, respectively. Currently, he is a lecturer of the School of Electrical Engineering of Xi'an University of Technology. His research interests include charge transport characteristics and mechanisms of polymer dielectric materials.



Zhe Hou received his Ph.D. degree from Xi'an Jiaotong University in 2017. Currently, he is working in the Electric Power Research Institute of State Grid Shaanxi Electric Power. His research interests include the detection of insulation status of distribution equipment.



Xi Chen received his M.S. degree from Xi'an University of Technology in 2021. His research interests include the insulation characteristics of dielectric materials in power systems and the insulation status detection of power grid equipment.



Zeli Ju holds a master's degree and is a senior engineer. Currently, he is working in the Electric Power Research Institute of State Grid Shaanxi Electric Power. His research interests include the operation, maintenance, and testing of power grid equipment for a long time.